THE JOURNAL OF BIOLOGICAL CHEMISTRY VOL. 290, NO. 1, pp. 612–624, January 2, 2015

In Vitro Reconstitution of Rab GTPase-dependent Vesicle Clustering by the Yeast Lethal Giant Larvae/Tomosyn Homolog, Sro7*

Received for publication, July 16, 2014, and in revised form, November 14, 2014 Published, JBC Papers in Press, November 17, 2014, DOI 10.1074/jbc.M114.595892

Guendalina Rossi[‡], Kelly Watson[‡], Mallory Demonch[‡], Brenda Temple[§], and Patrick Brennwald[‡1]

From the Departments of [‡]Cell Biology and Physiology and [§]Biochemistry and Biophysics, University of North Carolina at Chapel Hill, Chapel Hill, North Carolina 27599

Background: The mechanism by which Rab GTPases and their effectors act in tethering is not well understood.
Results: An *in vitro* assay was developed to study vesicle clustering by the Lgl family member Sro7.
Conclusion: Clustering *in vitro* and *in vivo* depends on the conformation of the Rab GTPase and Sro7.
Significance: This assay provides a new tool to dissect the role of Rab and Lgl family function.

Intracellular traffic in yeast between the Golgi and the cell surface is mediated by vesicular carriers that tether and fuse in a fashion that depends on the function of the Rab GTPase, Sec4. Overexpression of either of two Sec4 effectors, Sro7 or Sec15, results in the formation of a cluster of post-Golgi vesicles within the cell. Here, we describe a novel assay that recapitulates post-Golgi vesicle clustering *in vitro* utilizing purified Sro7 and vesicles isolated from late secretory mutants. We show clustering *in vitro* closely replicates the *in vivo* clustering process as it is highly dependent on both Sro7 and GTP-Sec4. We also make use of this assay to characterize a novel mutant form of Sro7 that results in a protein that is specifically defective in vesicle clustering both *in vivo* and *in vitro*. We show that this mutation acts by effecting a conformational change in Sro7 from the closed to a more open structure. Our analysis demonstrates that the N-terminal propeller needs to be able to engage the C-terminal tail for vesicle clustering to occur. Consistent with this, we show that occupancy of the N terminus of Sro7 by the t-SNARE Sec9, which results in the open conformation of Sro7, also acts to inhibit vesicle cluster formation by Sro7. This suggests a model by which a conformational switch in Sro7 acts to coordinate Rab-mediated vesicle tethering with SNARE assembly by requiring a single conformational state for both of these processes to occur.

We identified Sro7, the yeast member of the conserved family of Lgl proteins, in a screen for binding partners of the plasma membrane t-SNARE Sec9 (1). Loss of Sro7 and its redundant paralog Sro77 results in both cold-sensitive growth and a severe secretory defect in post-Golgi vesicle tethering/fusion with the plasma membrane (1). Importantly, Sro7 has been suggested to function as a direct effector of the GTPase Sec4 in a pathway that genetically appears to be parallel to that of the other effector of Sec4, the exocyst tethering complex (2). Although Sro7 has been found to interact with several components of the exocytic tethering and fusion apparatus (1, 3, 4), the precise molecular mechanism by which it functions in this process remains elusive. Structural analysis has shown that Sro7 is composed of two interlocking β-propellers with a long C-terminal tail that binds back to the N-terminal propeller in an autoinhibitory mode. The region bound by the tail was shown to overlap with the binding site of the plasma membrane t-SNARE Sec9 in a way that suggested the possibility of a "triggered" release of the SNARE by Sro7 (5). Although the Sec4 GTPase remained an attractive candidate triggering factor, its association with Sro7 had previously been shown to have no effect on Sro7's association with Sec9 (2). Therefore, the precise role of Sro7 as an effector of the Rab GTPase Sec4 remains elusive.

Overexpression of Sro7 in the cell results in the accumulation of a large cluster of post-Golgi vesicles and cell lethality (4). This observation was similar to that seen for another effector of the Sec4 GTPase, the Sec15 subunit of the exocyst tethering complex (6). *In vivo* analysis of the vesicle clustering phenotype showed that clustering and cell lethality by both Sec15 and Sro7 depend on Sec4 function but are independent of the Sec9 t-SNARE (4, 6). In the case of Sro7, vesicle clustering also depends upon the interaction between Sro7 and the type V myosin Myo2 (4).

In this study, we establish an *in vitro* assay that recapitulates the Sro7-mediated clustering we observed previously *in vivo*. Development of such an assay allows us to begin to biochemically dissect Rab GTPase and Rab effector function in parallel to our *in vivo* genetic analyses. We made use of this assay to analyze the effects of Sro7 mutants in which conserved charged patches on Sro7 were mutated to the reverse charge. We found that one of the charge reversal mutant proteins, Sro7-R189D,R222D, had a specific defect in clustering vesicles both *in vivo* and *in vitro*. Further analysis of this defect demonstrated a role for the "closed" conformation of the C-terminal autoinhibitory tail in vesicle clustering. This suggests a novel function for the conformational switch in Sro7 in coordinating Rab-dependent membrane tethering with regulation of SNARE assembly prior to membrane fusion.

* This work was supported, in whole or in part, by National Institutes of Health Grant GM-054712.
[1] To whom correspondence should be addressed: Dept. Cell Biology and Physiology, University of North Carolina at Chapel Hill, 522 Taylor Hall, Chapel Hill, NC 27599. Tel.: 919-8434995, E-mail: pjbrennw@med.unc.edu.

EXPERIMENTAL PROCEDURES

Plasmids Used—Single copy plasmids expressing Sro7 or charge reversal point mutations were obtained by site-directed mutagenesis on pB741 (*SRO7,CEN,* and *HIS3*). All *GAL-SRO7* constructs, previously subcloned into the integrating vector pB24 (*LEU2*) as BamHI-HindIII fragments, were then subcloned as BamHI-ApaI inserts into pB38 (*GAL, CEN,* and *HIS3*). Protein A-tagged Sro7 constructs were generated as BamHI-HindIII fragments in pB966 (2μ, *URA3*, plasmid containing the *ADH1* promoter and a protein A tobacco etch virus tag). Full-length Sec9 with an N-terminal GST tag and a C-terminal His_6 tag was obtained as described previously (7). Soluble GST-Snc1, GST-Sso1, and GST-Sso1(193–265) were obtained by standard glutathione elution of the fusion protein from glutathione-Sepharose beads following the manufacturer's directions (GE Healthcare). Plasmid for recombinant GDI[2] production, pGDI-CBD, was a gift of V. Starai and was used as described (8).

Protein Purification—Sro7 with an N-terminal Protein A tag was obtained from a modification of the purification protocol described previously (2). Sro7 was expressed behind an *ADH1* promoter from a high copy plasmid in a yeast *pep4*Δ background strain. Approximately 5 liters of cells were grown overnight in synthetic media to an A_{599} of 3.0 and then shifted to YP + 2% glucose for one doubling time. Cells were then harvested and washed in 200 ml of ice-cold buffer containing 10 mM Tris, pH 7.8, 20 mM sodium azide, and 20 mM sodium fluoride to yield a final wet weight of ~50 g of cells. Cells were frozen on dry ice and stored at −80 °C. Lysis was obtained with a bead beater using ice-cold buffer containing 20 mM Tris, pH 7.8, 150 mM NaCl, 0.5% Tween 20, and 1 mM DTT, and protease inhibitors (2 μg/ml leupeptin, 2 μg/ml aprotinin, 2 μg/ml antipain, 14 μg/ml pepstatin A, and 1 mM phenylmethylsulfonyl fluoride). Five cycles of 1-min bead beating, followed by 2-min intervals on ice were used to lyse the cells. The lysate (60 ml) was then spun at 17,400 × *g* for 10 min at 4 °C in a JA 25.5 rotor before further dilution (120 ml) and ultracentrifugation at 140,000 × *g* for 30 min at 4 °C in a type 45Ti rotor to yield a final protein concentration of about 25 mg/ml. Binding to Sepharose CL-6B beads (1 ml of beads/45 ml of lysate) for 1 h at 4 °C was then used to preclear the lysate before binding to 1 ml of IgG-Sepharose beads for 2 h at 4 °C. Beads were then washed five times with lysis buffer, three times with lysis buffer containing 400 mM NaCl, and three times with ice-cold cleavage buffer containing 20 mM Tris, pH 7.8, 150 mM NaCl, 0.1 mM EDTA, and 1 mM DTT. Beads were then resuspended 1:1 in cleavage buffer, and cleavage was obtained with tobacco etch virus cleavage enzyme for 5 h at 17 °C (5000 units of tobacco etch virus/3-ml bed volume beads). Supernatant containing the cleaved protein was then collected and frozen at −80 °C.

Vesicle Enrichment—Yeast mutant cells grown overnight in YP + 2% glucose to an A_{599} of 0.6 were shifted to the restrictive temperature of 37 °C for 2 h. Sodium azide was then added (final 20 mM) to the culture, and 300 absorbance units were centrifuged, washed with 10 ml of 10 mM Tris, pH 7.5, 20 mM NaN_3, and spheroplasted in 10 ml of spheroplast buffer (0.1 M Tris, pH 7.5, 1.2 M sorbitol, 10 mM NaN_3, 21 mM β-mercaptoethanol, and 0.05 mg/ml Zymolyase 100T) for 30 min at 37 °C. Spheroplasts were then lysed in 4 ml of ice-cold lysis buffer (10 mM triethanolamine, pH 7.2, 0.8 M sorbitol) with protease inhibitors (2 μg/ml leupeptin, 2 μg/ml aprotinin, 2 μg/ml antipain, 14 μg/ml pepstatin A, and 1 mM phenylmethylsulfonyl fluoride). The yeast lysate was then centrifuged at 450 × *g* for 4 min at 4 °C to remove unbroken cells, and the remaining lysate was spun at 30,000 × *g* for 15 min at 4 °C in a Sorvall centrifuge to pre-clear larger membranes. Approximately 2.5 ml of supernatant was then labeled with FM4-64 (1 μg/ml) for 10 min on ice. The labeled lysate was then layered over 2 ml of an ice-cold sorbitol cushion (20% w/v sorbitol in 10 mM triethanolamine, pH 7.2) and centrifuged at 100,000 × *g* for 1 h at 4 °C. After removal of the supernatant fraction, the pellet fraction was resuspended in 600 μl of lysis buffer and kept on ice for use in the clustering assay. When the *sec4-8* secretory mutant was used the following adjustments were made: 600 absorbance units were harvested and spheroplasted in 15 ml of spheroplast buffer. The final 100,000 × *g* pellet fraction was resuspended in 700 μl of lysis buffer. To obtain an enriched vesicle fraction from the *sec6-4* mutant expressing GFP-Sec4 (*CEN),* cells grown overnight in selective media were first shifted to YP + 2% glucose at 25 °C for 1 h before placing them at the restrictive temperature of 36 °C for 2 h. 350 absorbance units were spheroplasted with 10 ml of spheroplast buffer and treated as above except the 100,000 × *g* pellet was resuspended in 350 μl of lysis buffer. To obtain an enriched vesicle fraction from the *snc1*Δ; *snc2*Δ *GAL*-depletion strain, where the sole source of Snc1 is under the control of the *GAL1/10* promoter, cells were grown in YP + 2% glucose and then shifted to YP + 3% raffinose for 14 h before harvesting 700 absorbance units that were then spheroplasted, lysed, and subjected to centrifugation as described for the *sec6-4* mutant strain. The final high speed pellet fraction was resuspended in 160 μl of lysis buffer.

Vesicle Purification—To obtain a homogeneous population of post-Golgi vesicles, the 100,000 × *g* pellet, obtained as described above in the vesicle enrichment section, was subjected to a 20–40% sorbitol velocity gradient (9). Adjustments to the above protocol included harvesting 700 absorbance units of cells and resuspending the 100,000 × *g* pellet in a final volume of 600 μl prior to loading at the top of 11 ml of linear sorbitol gradient prepared with 1.22-ml steps of 40, 37.5, 35, 32.5, 30, 27.5, 25, 22.5, and 20% sorbitol (w/v) in 10 mM triethanolamine acetate, pH 7.2. The gradient was centrifuged at 71,000 × *g* for 80 min at 4 °C and then fractionated into 0.72-μl fractions. Fractions 5–7 (pink color) containing the vesicle fractions were then pooled, diluted with 3 ml of lysis buffer, and centrifuged at 100,000 × *g* for 1 h. The pellet fraction containing the purified vesicles was resuspended in 200 μl of lysis buffer. For vesicle purification from the *sec4-8* mutant strain, the above protocol was adjusted by using 1000 absorbance units of mutant cells and spheroplasting with 25 ml of spheroplast buffer. The spheroplasts were then lysed with the same volume (9 ml) as the *sec6-4* mutant cells, and the 100,000 × *g* pellet was resuspended in 600 μl and loaded on a 20–40% sorbitol velocity gradient as described above. The sample was treated identi-

[2] The abbreviations used are: GDI, GDP dissociation inhibitor; HSP, high speed pellet; GTPγS, guanosine 5′-3-*O*-(thio)triphosphate; TRITC, tetramethylrhodamine isothiocyanate.

cally to the *sec6-4* mutant strain for the final concentration of the purified vesicle fraction.

GDI Extraction and Vesicle Purification—For the GDI-treated vesicles, the following modifications were made to the vesicle enrichment protocol described above: 1400 absorbance units of a *sec6-4* mutant strain were grown overnight and shifted to the restrictive temperature of 37 °C for 2 h. The final high speed pellet fraction was resuspended into 1 ml of lysis buffer and treated with 0.5 mM GDP and 3.6 mM $MgCl_2$ for 30 min on ice. The vesicles were then split into two 500-μl aliquots that were treated with 8 mM GDI or mock-treated with buffer only for 30 additional min on ice. Lysis buffer was then added to bring each volume to 600 μl before loading onto two separate but identical 20–40% sorbitol velocity gradients for vesicle purification. Vesicle-containing fractions from each gradient were then pooled, concentrated by a high speed centrifugation at 100,000 $\times$ *g* as described in the vesicle purification protocol, and resuspended in a final volume of 150 μl before using in the *in vitro* clustering assay.

Antibody Inhibition of Vesicle Clustering in Vitro—For the antibody inhibition studies, a, HSP fraction obtained from a *sec6-4* mutant strain was incubated with equal amounts of monoclonal anti-Sec4 or control monoclonal anti-Myc for 1 h on ice before treating with $MgCl_2$ (3 mM) and nucleotide (1 mM) for 30 additional min on ice. The vesicles were then incubated with Sro7 (1 μM) for 20 min at 27 °C.

Clustering Assay—Vesicle-enriched fraction or purified vesicles (10 μl) were preincubated with $MgCl_2$ (3 mM) and nucleotide (1 mM) for 30 min on ice prior to addition of Sro7 (1 μM) or mock buffer for 20 min at 27 °C.

Negative Staining—The carbon film grids were glow-discharged in a Harric Plasma Cleaner for 1.5 min. A drop of sample (10 μl) was placed onto a grid that was suspended in reverse forceps for 1 min. The sample was then washed off with 5 drops of 1% aqueous uranyl acetate. The stain was allowed to sit on the grid for 1 min. The grid was blotted on the tip of the forceps with filter paper before air drying and was examined by electron microscopy.

Immunofluorescence—Strains containing a *CEN* vector (pB38) expressing wild type *SRO7*, *sro7-R189D,R222D,* or *sro7-K914,F942* from a *GAL*-inducible promoter were grown overnight in synthetic media with raffinose (3%) to early log phase and then induced with 1% galactose for 6 h before fixing and processing as described previously (10).

Binding Assays—Bindings of wild type Sro7 or point mutant forms of Sro7 were set up as described previously (7) for Sec9-Qbc, Exo84-NT (amino acids 3–400), and Myo2-IQ (amino acids 782–990). Bindings to GTP-Sec4 made use of procedures described in Ref. 2. To compare wild type Sro7 to point mutant forms of Sro7, two different sets of soluble protein concentrations were used to ensure the binding response was in a linear range. Student's *t* test was done on three individual bindings for each protein concentration used.

RESULTS

Sro7-dependent Vesicle Clustering in Vitro Requires Magnesium Chloride and Is Potentiated by GTPγS—We have previously shown that overexpression of *SRO7* behind a *GAL1/10* promoter results in a pronounced growth defect and the formation of a large cluster of post-Golgi vesicles within the cell (4). Importantly, this clustering is dependent on GTP-Sec4 as mutations in *SEC4* and the gene encoding its exchange factor *SEC2* prevent clustering of vesicles when Sro7 is overexpressed (4, 11). To further explore how Sro7 mediates vesicle clustering, we sought to determine whether we could recapitulate this process *in vitro* utilizing isolated post-Golgi vesicles and purified Sro7 protein. Sro7 was purified from yeast by a modification of a previous protocol used in the laboratory (2), and post-Golgi secretory vesicles were isolated from a *sec6-4* mutant strain that accumulates a large number of vesicles following a shift to the restricted temperature of 37 °C (12, 13). To visualize vesicles in the assay, they were fluorescently labeled by two methods. In the first method, vesicles were labeled *in vivo* by expression of GFP-Sec4 in a *sec6-4* strain, and Sec4 is a well recognized marker of post-Golgi secretory vesicles (14). In the second method, vesicles were labeled *in vitro* with the lipid dye FM4-64 during the vesicle isolation procedure. In both cases, post-Golgi vesicles were isolated by cell fractionation following a shift of the mutant *sec6-4* strain to the restrictive temperature.

To determine whether we could reconstitute Sro7-mediated vesicle clustering *in vitro*, fluorescently labeled vesicle fractions were incubated with increasing amounts of purified Sro7 under a number of different conditions. Following a 20-min incubation at room temperature, an aliquot of each condition was analyzed by fluorescence microscopy. Clustering appeared as the formation of fluorescently labeled puncta that were observed using either FITC (GFP-Sec4-labeled vesicles) or TRITC (for FM4-64 labeled vesicles) filter sets. Note individual post-Golgi vesicles (80–100 nm) were too small to be visualized by conventional fluorescence microscopy. When purified Sro7 was added to vesicles in buffer containing GTPγS and magnesium, large puncta formed that were visible by both FITC and TRITC channels (Fig. 1*A*). The appearance of large puncta depended on the presence of Sro7, magnesium, and GTPγS. In the absence of either magnesium or Sro7, no puncta formed. Similarly, when BSA or IgG was added in place of Sro7 (at equivalent amounts), no clustering was observed (data not shown). When Sro7 and magnesium were present with GDP in place of GTPγS or no added nucleotide was present, then only small puncta formed (Fig. 1*A*). Finally, we found that the clustering was dependent on both time and the dose of Sro7, as the size of puncta increased with time and with increasing amounts of Sro7 added (data not shown). Routine assays were done with the addition of Sro7 to 1 μM incubated with vesicles for 20 min at 27 °C. Clustering activity was quantitated by counting the number of small (greater than 1 μm but less than 2 μm) and larger (>2 μm) clusters formed per 1 μl of assay mix (Fig. 1*B*).

GTP-bound Sec4 Is Required for Sro7-mediated Vesicle Clustering in Vitro—To determine whether the *in vitro* clustering was also dependent on Sec4, we prepared FM4-64 labeled secretory vesicles from a number of late secretory mutants (*sec6-4*, *sec4-8*, *sec1-1*, and *sec9-4*) and examined the ability of purified Sro7 to induce vesicle clustering under the conditions described above. To ensure we had similar numbers of vesicles present from each mutant strain, we used immunoblots of the vesicle fractions used in this assay to monitor levels of three vesicle markers Sec4, the v-SNARE, Snc1/2, and the t-SNARE,

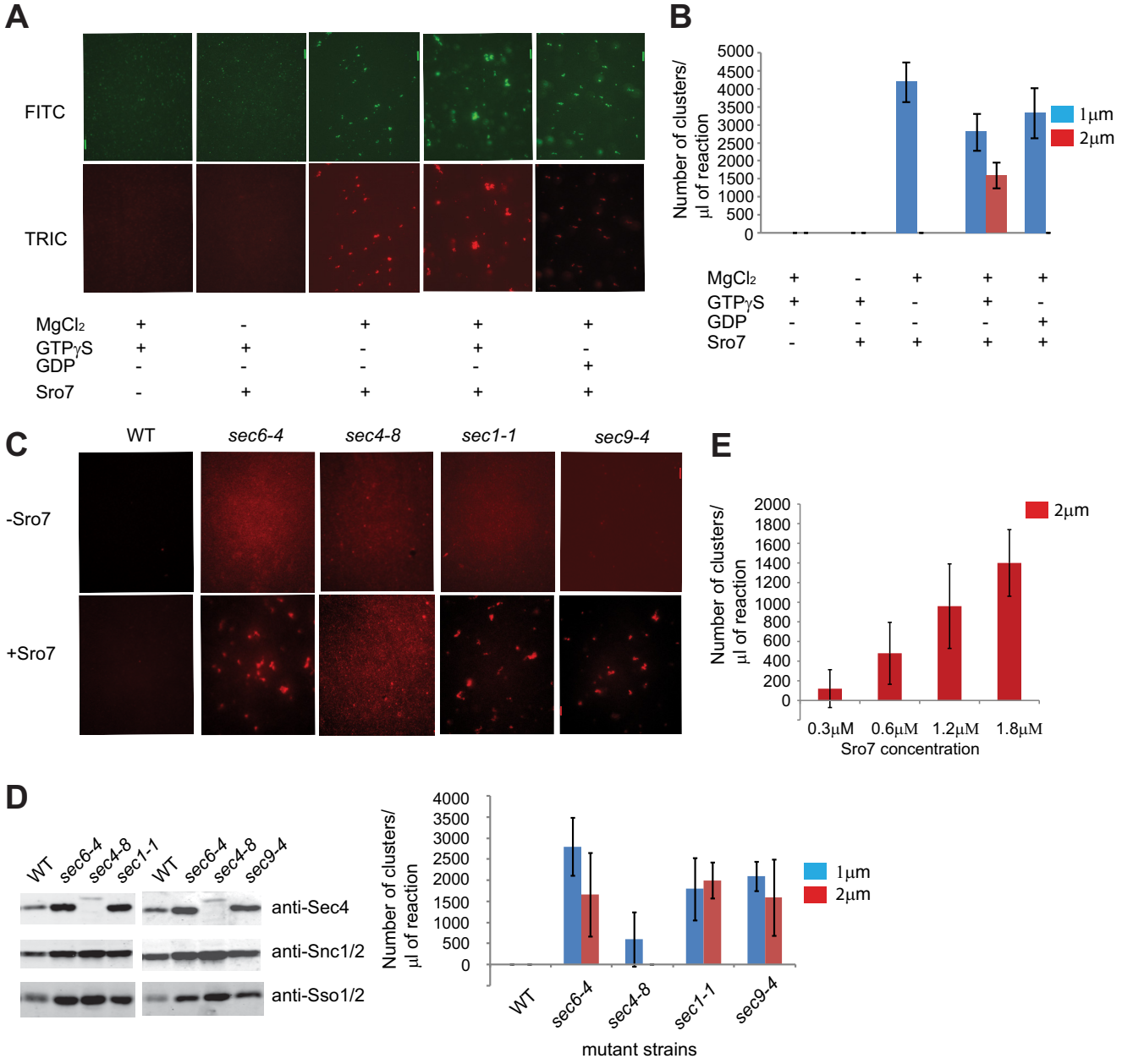

FIGURE 1. ***In vitro* system for clustering post-Golgi vesicles in the presence of Sro7, $MgCl_2$, and GTPγS.** *A*, *sec6-4* mutant strain expressing GFP-Sec4 (*CEN*) was shifted to the restrictive temperature of 37 °C to accumulate post-Golgi vesicles. The mutant cells were then spheroplasted, lysed, and spun at 30,000 × *g* to remove large membranes. The supernatant was then labeled with FM4-64 and spun at 100,000 × *g* over a sorbitol cushion to generate a concentrated HSP fraction enriched in post-Golgi secretory vesicles. The HSP fraction was then treated with or without $MgCl_2$ (3 mM), GTPγS, or GDP (1 mM) for 30 min on ice, and then Sro7 (1 μM) was added for 20 min at 27 °C. A 1-μl aliquot of the reaction mixture was analyzed by fluorescence microscopy, and quantitation of vesicle cluster formation (*B*) was based on counting 10 images at ×60 magnification and separating vesicle clusters by size. *Scale bar,* 2 μm. *C*, post-Golgi vesicle fractions (HSP) labeled with FM4-64 were obtained as above from WT, *sec6-4*, *sec4-8*, *sec1-1*, and *sec9-4* mutant strains. HSP fractions from the different strains were then treated with $MgCl_2$ (3 mM) and GTPγS (1 mM) for 30 min on ice and then with Sro7 (1 μM) for 20 min at 27 °C. *D,* total vesicle material (HSP) was monitored by Western blot analysis with vesicle marker proteins (Sec4, Snc1/2, and Sso1/2), and quantitation of *in vitro* clustering was obtained as in *A*. *Scale bar,* 2 μm. *E*, vesicle clustering in a *sec6-4* HSP fraction labeled with FM4-64 increased with the concentration of Sro7 used in the assay.

Sso1/2 (which transits to the plasma membrane on post-Golgi vesicles). As expected, the vesicles from *sec4-8* have only a small amount of a form of Sec4 with altered mobility on SDS-PAGE (14) but have similar amounts of Snc1/2 and Sso1/2 when compared with the other three mutants (Fig. 1*D*). When these four vesicle preparations were incubated with Sro7 under the conditions described above, robust clustering was observed for *sec6-4*, *sec1-1*, and *sec9-4* vesicle fractions, but only low levels of small puncta were observed for the *sec4-8* vesicle fraction (Fig. 1*C*). The clustering activity of Sro7 was dose-dependent (Fig. 1*E*). Therefore, similar to the *in vivo* clustering, the *in vitro* clustering reaction was dramatically impeded with otherwise equivalent vesicles isolated from a *sec4-8* mutant strain.

To further rule out a role for SNARE proteins in Sro7-mediated vesicle clustering, we prepared vesicles from strains deficient in either Snc1/2 or Sso1/2 (15, 16). Using post-Golgi vesicles isolated from a strain where the sole source of Snc1 was under control of the *GAL1/10* promoter, we found that cluster-

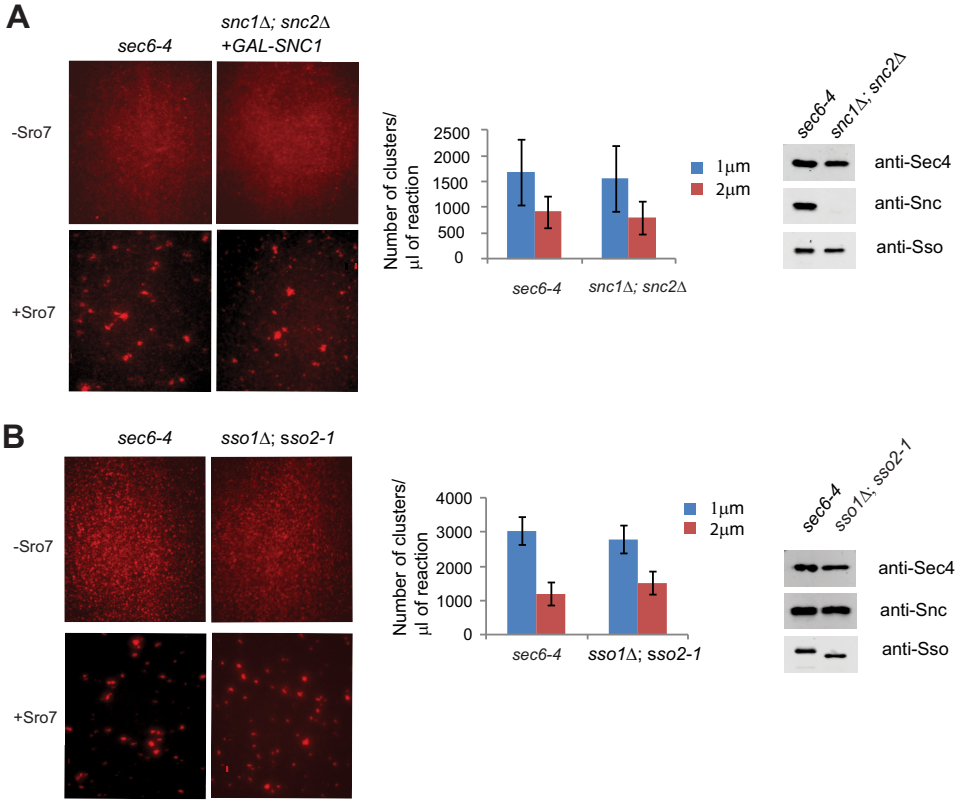

FIGURE 2. **Post-Golgi vesicles do not require functional SNARE proteins, Snc1/2 or Sso1/2, to cluster *in vitro* in the presence of Sro7, $MgCl_2$, and GTPγS.** *A*, *sec6-4* mutant strain was shifted to the restrictive temperature of 37 °C to accumulate post-Golgi secretory vesicles and then spheroplasted, lysed, and fractionated as described in Fig. 1 to obtain an HSP fraction enriched in labeled post-Golgi vesicles for the clustering assay. Vesicles depleted of the v-SNARE Snc1/2 were generated by shifting a *snc1*Δ;*snc2*Δ strain expressing *GAL-SNC1* from YP + 2% glucose into YP + 3% raffinose for 14 h at room temperature before processing as seen for the *sec6-4* mutant strain. Vesicle amounts from the two strains were normalized by Western blot analysis of vesicle marker proteins (Sec4, Snc1/2, and Sso1/2). Vesicle fractions were incubated with $MgCl_2$ (3 mM) and GTPγS (1 mM) for 30 min on ice and then treated with Sro7 (1 μM) for 20 min at 27 °C before analysis by fluorescence microscopy as described in Fig. 1. *B*, *sec6-4* and a *sso1*Δ;*sso2-1* secretory mutant strain were grown at room temperature and then shifted to 37 °C to accumulate post-Golgi vesicles. Strains were spheroplasted, lysed, and subjected to differential centrifugation to obtain an HSP fraction enriched in vesicles that were normalized using Western blot analysis of vesicle marker proteins. The *in vitro* assay was then conducted and quantitated as described in Fig. 1. *Scale bar,* 2 μm.

ing activity was unaffected, although the amounts of Snc1 on the vesicles were virtually undetectable (Fig. 2*A*). Likewise, when vesicles were isolated from the temperature-sensitive *sso1*Δ,*sso2-1* strain, we found Sro7-mediated clustering to be indistinguishable from that seen with vesicles from a *sec6-4* strain (Fig. 2*B*). Taken together with the results from the *sec9-4* strain, it is clear that post-Golgi SNARE function was not required for Sro7-mediated vesicle clustering.

The assay described above makes use of a high speed pellet fraction produced from differential centrifugation as a highly enriched source of post-Golgi vesicles (13). To determine whether purified post-Golgi vesicles are active in Sro7-mediated clustering, we subjected the FM4-64-labeled vesicle-enriched fraction to velocity sedimentation on sorbitol gradients (9). Vesicle purification was performed in parallel on both *sec6-4* and *sec4-8* mutant strains and examined under conditions identical to those described above, except that clustering reactions were allowed to incubate for 60 rather than 20 min to achieve similar levels of clustering as monitored by fluorescence microscopy (Fig. 3, *A* and *B*). The use of velocity gradient-purified vesicles of homogeneous size also allowed us to examine the clustering reactions by negative stain electron microscopy. The results, shown in Fig. 3*C*, demonstrate that Sro7 induces clustering, but not fusion, of purified 80–100-nm post-Golgi vesicles and that this clustering depends on both GTPγS and Sec4 function. Both Western blot quantitation of Snc1/2 levels and negative stain analysis of the purified vesicles demonstrate that equivalent numbers of *sec6-4* and *sec4-8* vesicles were used in this analysis (Fig. 3, *C* and *D*). Importantly, the quantification of vesicle clustering observed by electron microscopy is remarkably similar to the data obtained by quantification of the clustering reaction by fluorescence microscopy, indicating that both methods of visualizing clustering are indeed measuring the same event.

The Sec4 GTPase can cycle on and off membranes in a manner that is dependent on the nucleotide state of the Rab and its interaction with GDI (17). To determine whether the absence of clustering seen with the *sec4-8* secretory vesicles correlated with a loss of Sec4 function and not with an indirect defect in the *sec4-8* mutation on the functionality of the vesicles, we made use of purified recombinant Rab GDI to extract Rab GTPases from the vesicles. Secretory vesicle-enriched fractions were generated from *sec6-4*, pretreated with GDP, and followed by either extraction with recombinant Rab GDI or mock-treated with buffer only before further purification on sorbitol gradients. Treatment with Rab GDI resulted in the removal of

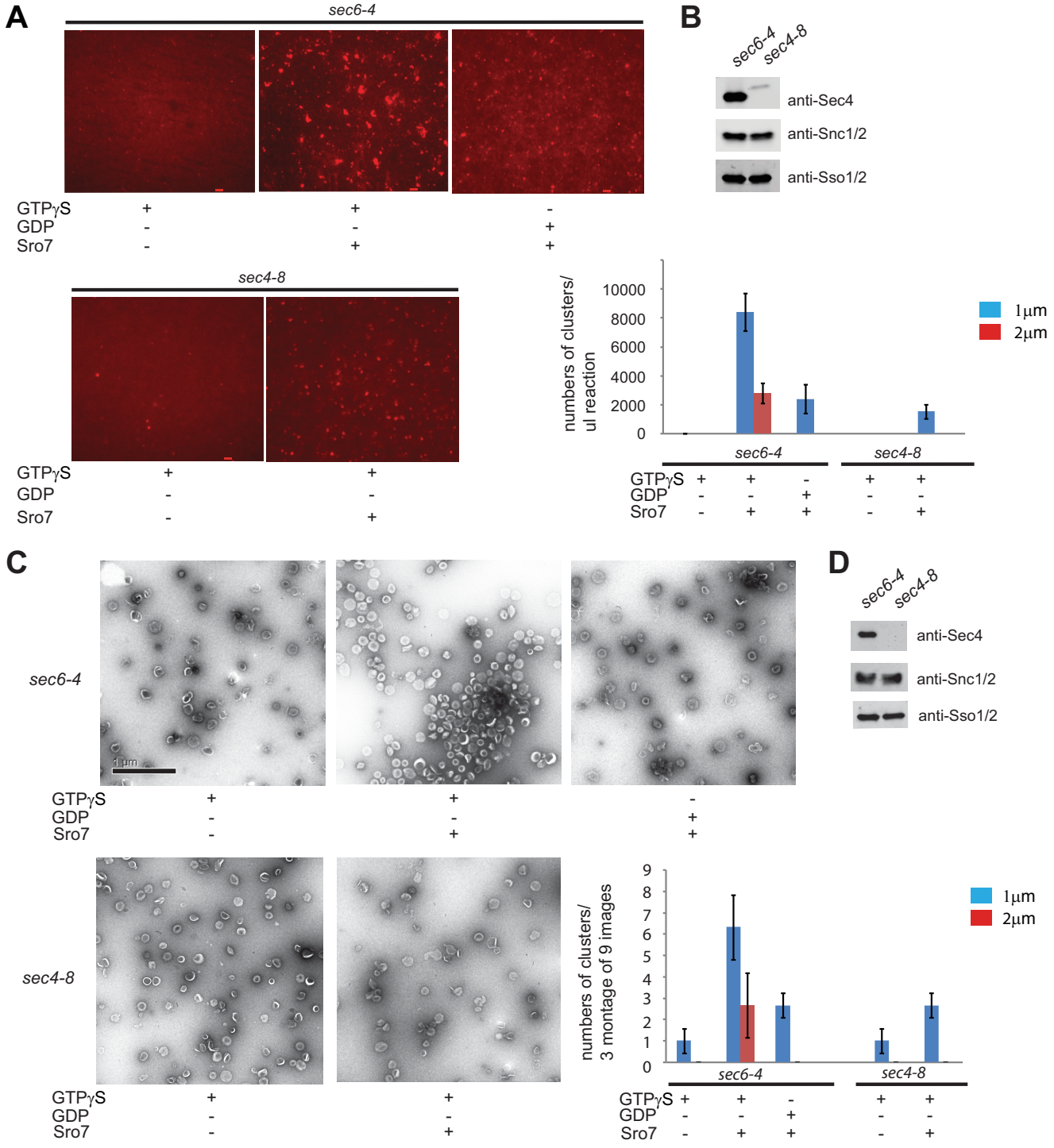

FIGURE 3. **Purified post-Golgi vesicles cluster *in vitro* in the presence of Sro7, $MgCl_2$, and GTPγS.** *A*, *sec6-4* and *sec4-8* mutant strains were shifted to the restrictive temperature of 37 °C to accumulate secretory vesicles. Cells were then spheroplasted, lysed, and subjected to a 30,000 × *g* spin to remove large membranes. The lysates were then treated with FM4-64 and spun through a sorbitol cushion at 100,000 × *g* to generate two HSP fractions that were then subjected to parallel 20–40% sorbitol velocity gradients. Vesicle-containing fractions were collected from each gradient and subjected to a second 100,000 × *g* centrifugation to generate a homogeneous fraction of *sec6-4* or *sec4-8* vesicles. These were then treated with $MgCl_2$ (3 mM) and GTPγS (1 mM) for 30 min on ice and then with Sro7 (1 μM) for 60 min at 27 °C. Clustering was analyzed both by fluorescence microscopy (*A*) and negative stain electron microscopy (*C*). HSP fractions of purified vesicles were monitored by Western blot analysis (*B* and *D*), and quantitation of vesicle clustering for *A* was based on counting 10 images at ×60 magnification and separating vesicle clusters by size. *Scale bar*, 2 μm. Quantitation for *C* was based on counting three montages of nine frames each.

nearly ⅔ of the Sec4 from vesicles (Fig. 4*C*). The vesicles were then used in the *in vitro* clustering assay with Sro7, magnesium chloride, and GTPγS. Although overall clustering was slightly reduced following the more extensive incubations necessary for GDI extraction (compare quantitation in Fig. 3*B* to 4*B*), the observed clustering in the mock-treated vesicles was dependent on Sro7. Importantly, the results shown in Fig. 4, *A* and *B*, demonstrate that GDI treatment of the secretory vesicles

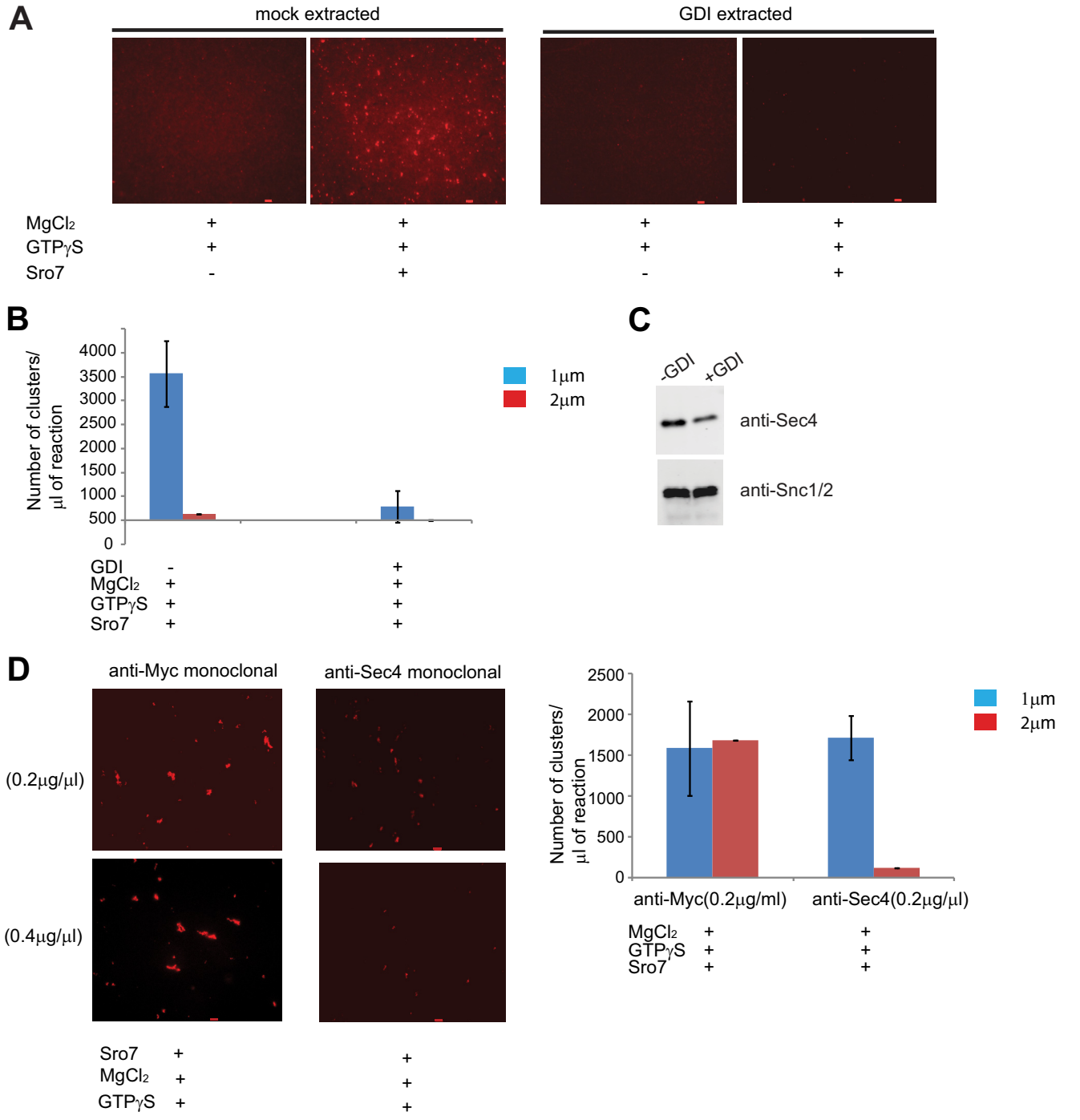

FIGURE 4. ***In vitro* post-Golgi vesicle clustering depends on the presence of GTP-Sec4 on vesicles.** *A*, HSP fraction obtained from a *sec6-4* mutant strain was treated with GDP (0.5 mM), $MgCl_2$ (3.6 mM, and GDI (8 mM) or a mock buffer for 30 min on ice. The vesicles were then purified on parallel 20–40% sorbitol velocity gradients. Vesicle-containing fractions from each column were subject to a second centrifugation to generate two concentrated vesicle fractions. GDI-treated and mock-treated samples were then incubated with $MgCl_2$ (3 mM) and GTPγS (1 mM) on ice for 30 min and then with Sro7 (1 μM) for 60 min at 27 °C. Results of the clustering assay were analyzed by fluorescence microscopy (*A*), and quantitation of clustering is shown in *B*. *Scale bar,* 2 μm. Vesicle amount used was monitored by Western blot analysis (*C*) using polyclonal antibody to vesicle markers Sec4 and Snc1/2. *D*, HSP fraction obtained from a *sec6-4* mutant strain was incubated with equal amount of monoclonal anti-Sec4 or control monoclonal anti-Myc IgG for 1 h on ice before treating with $MgCl_2$ (3 mM) and GTPγS (1 mM) for 30 additional min on ice. The vesicles were then incubated with Sro7 (1 μM) for 20 min at 27 °C. The reaction was analyzed by fluorescence microscopy and quantitated as described previously. *Scale bar,* 2 μm.

results in a dramatic loss of the clustering potential of the purified vesicles.

Rab GDI is known to have high specificity for Rab GTPases (18); however, yeast post-Golgi vesicles are known to contain several other Rab GTPases, including Ypt31 and Ypt1, which could be responsible for the GDI-mediated inhibition in the assay (19–21). Therefore, to determine whether Sec4 is the relevant Rab in this assay, we made use of a monoclonal antibody specific to Sec4 (22) as a functional probe for Sec4 function *in vitro*. We treated *sec6-4* vesicles in a high speed pellet vesicle

fraction with two different doses of either anti-Sec4 mAb or an identical amount of a control mAb. Both antibodies were purified and used at identical concentrations in the assay by preincubating them with vesicles for 1 h on ice prior to use in the clustering assay. The results in Fig. 4*D* show that vesicles treated with the anti-Sec4 monoclonal antibody, but not those treated with the control antibody, demonstrated a pronounced dose-dependent inhibition of clustering. Taken together with the data obtained with *sec4-8* vesicles and Rab GDI extraction studies, this result provides strong evidence that Sec4 on the surface of the post-Golgi vesicles is critical for Sro7-mediated vesicle clustering.

Novel Mutant, Sro7-R189D,R222D, Fails to Cluster Post-Golgi Vesicles in Vivo and in Vitro—To identify elements within Sro7 that are important for vesicle tethering, we carried out a small pilot screen of site-specific mutations in conserved surface patches and examined their effect on Sro7-mediated vesicle clustering *in vivo* and *in vitro*. Reverse charge mutagenesis of four conserved surface "patches" of charged amino acids resulted in four new mutants shown in Fig. 5*A*. All four mutants were fully functional as the only copy of Sro7 in the cell when expressed behind the endogenous Sro7 promoter (data not shown). As a first attempt to determine whether any of these mutants affect post-Golgi vesicle clustering, we introduced each allele into a *GAL1/10* expression plasmid and examined the growth effects following induction on galactose-containing media. As we have previously shown, *GAL* overexpression of wild type *SRO7* results in a significant growth defect in wild type strains (4). Although three of the four charge reversal mutants demonstrated pronounced growth defects, one of the mutants, *sro7-R189D,R222D* (abbreviated as *sro7-D189,D222*), did not cause cell lethality when overexpressed in wild type or a more sensitive *sec* mutant strain, *sec15-1,* in which exocyst function is compromised (Fig. 5*B*). To understand the biological basis for the loss of growth inhibition, we determined the effect of the expression of this allele on post-Golgi vesicle clustering by immunofluorescence microscopy. As we have observed previously, *GAL* induction of *SRO7* results in large puncta of Sec4- and Sro7-positive structures that correspond to clusters of 80–100-nm vesicles by thin section electron microscopy (Fig. 5*C*) (4). In contrast, when we induced expression of *sro7-D189,D222*, no puncta were observed by either Sec4 or Sro7 staining. Moreover, the normally highly polarized staining of Sec4 appeared to be replaced often by a much more diffuse staining pattern, although there is no effect on growth under these conditions (Fig. 5*C*).

To compare the clustering activity of the *sro7-D189,D222* mutant *in vitro* to the *in vivo* results described above, we purified the mutant protein to homogeneity and examined its ability to promote clustering in our assay. Although the mutant protein shows no detectable effect on binding to GTP-Sec4 (Fig. 6*B*), it completely fails to stimulate vesicle clustering of both FM4-64-labeled (Fig. 6*A*) or GFP-Sec4-labeled vesicles (data not shown) isolated from *sec6-4* strains. Furthermore, the clustering defect cannot be ascribed to a defect in the interaction with Myo2 (7) or Exo84 (3) because we find binding of the purified Sro7-D189,D222 protein to recombinant forms of Myo2 and Exo84 is indistinguishable from that of the wild type Sro7 protein (Fig. 6*C*).

Examination of the arginine residues at positions 189 and 222 in the Sro7 crystal structure indicates that these residues, which lie on the surface of the N-terminal β-propeller, play an important role in the interaction with the C-terminal autoinhibitory tail (Fig. 5*A*). The autoinhibitory tail is thought to regulate interaction of Sro7 with the Qbc-SNARE domain of the plasma membrane t-SNARE, Sec9 (5). To test the idea that the effect of the Asp-189 and Asp-222 mutations on clustering is through loss of the autoinhibitory interaction of the C-terminal domain with the propeller, we generated an additional set of mutations (N914K and S942F) in the C-terminal tail, which form strong hydrogen bond interactions with the two arginine residues on the N-terminal propeller (Fig. 7*A*). To test the structural prediction that the autoinhibitory tail would be in a more "open" conformation in both the Sro7-D189,D222 and Sro7-K914,F942 mutant proteins, we examined their ability to bind the Sec9-Qbc domain fused to GST. The results, shown in Fig. 7*B*, demonstrate that both of these mutant proteins show significantly improved binding to GST-Sec9Qbc compared with equivalent quantities of wild type Sro7.

To determine whether the *sro7-K914,F942* mutant, like the *sro7-D189,D222* mutant, suppresses the vesicle clustering phenotype *in vivo*, we expressed this mutant behind the *GAL* promoter. The results in Fig. 7*C* show that this new allele, like the *sro7-D189,D222*, prevents the galactose-dependent inhibition of growth. Importantly, we also find that *GAL* induction of this allele prevents formation of the large Sec4 positive vesicle clusters seen with wild type Sro7 (Fig. 7*D*). Finally, we determined whether the purified Sro7-K914,F942 protein had reduced activity in the *in vitro* vesicle clustering assay by comparing it with the wild type Sro7 and the Sro7-D189,D222 mutant. The results in Fig. 8*A* demonstrate that the two mutant forms of Sro7 are completely inactive for *in vitro* vesicle clustering, despite the fact they show normal binding to Myo2, Exo84, and enhanced binding to Sec9-Qbc.

These data strongly suggest that the closed form of Sro7, where the C-terminal autoinhibitory tail is engaged with the N-terminal propeller, is most active in Rab-dependent vesicle clustering. Because the closed conformation is mutually exclusive with binding of the Sec9-Qbc domain to Sro7, we asked whether prebinding of Sro7 to excess full-length Sec9 protein would affect the clustering activity of otherwise wild type Sro7. The results of this experiment, shown in Fig. 8*B*, demonstrate that binding of Sec9 to Sro7 in the assay potently inhibited vesicle clustering by Sro7, exactly as predicted by this model. The inhibition by Sec9 is dose-dependent (Fig. 8*D*) and specific in that neither the cytoplasmic domain of Sso1 nor Snc1 showed any effect in the assay (Fig. 8, *B* and *C*). Also consistent with the notion that Sec9 inhibition is through binding to Sro7, we find that eliminating the prebinding incubation step significantly reduced the inhibitory effect of Sec9 on Sro7-mediated clustering (data not shown). Taken together, we find that "opening" the autoinhibitory tail by three different means, propeller mutant, tail mutants, or Sec9 binding, all lead to inhibition of clustering activity. This suggests that the binding of the autoinhibitory tail acts as a "switch" to coordinate Sro7 function in

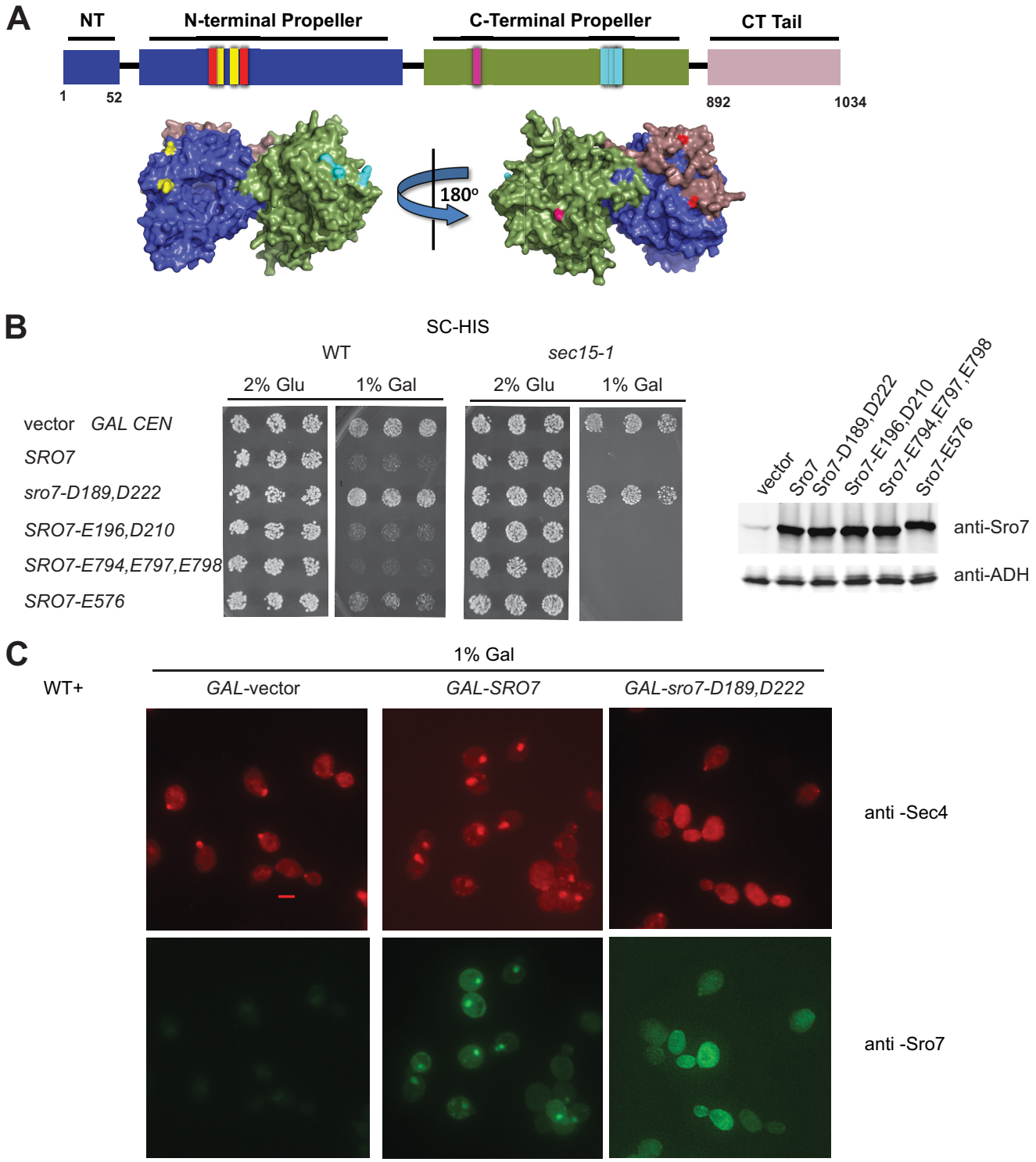

FIGURE 5. **Novel mutant of Sro7, *sro7-R189D,R222D* fails to induce clustering and cell lethality *in vivo*.** *A*, schematic and surface-filling model show the four new, surface-exposed, conserved charge-reversal Sro7 mutants as follows: *red*, *Sro7-R189D,R222D*; *yellow*, *Sro7-K196E,R210D*; *light blue*, *Sro7-K794E,H797E,K798E*; *violet*, *Sro7-K576E*. *B*, wild type and *sec15-1* mutant strains were transformed with plasmids, (*CEN*) overexpressing Sro7, or the charge reversal mutants from a *GAL* promoter. Three individual colonies were picked and transferred to selective media in the presence of glucose or galactose. Equal absorbance units of the strains induced in galactose were harvested, washed in Tris (10 mM) and azide (20 mM), and lysed by glass bead lysis before subjecting to Western blot analysis. *C*, wild type cells containing plasmids expressing *SRO7* or *sro7-D189,D222* from a *GAL*-inducible promoter (*CEN*) or vector only were grown in selective media and induced for 6 h in galactose before fixing and processing for immunofluorescence analysis using monoclonal Sec4 and polyclonal Sro7 antibodies. *Scale bar*, 2 μm.

Rab-dependent membrane tethering and SNARE assembly. Although the precise order of events necessary to turn this switch will need to be sorted out, one attractive model would be that closure of the autoinhibitory tail would act to temporally regulate Rab-mediated vesicle tethering with SNARE assembly necessary for subsequent fusion (Fig. 8*E*).

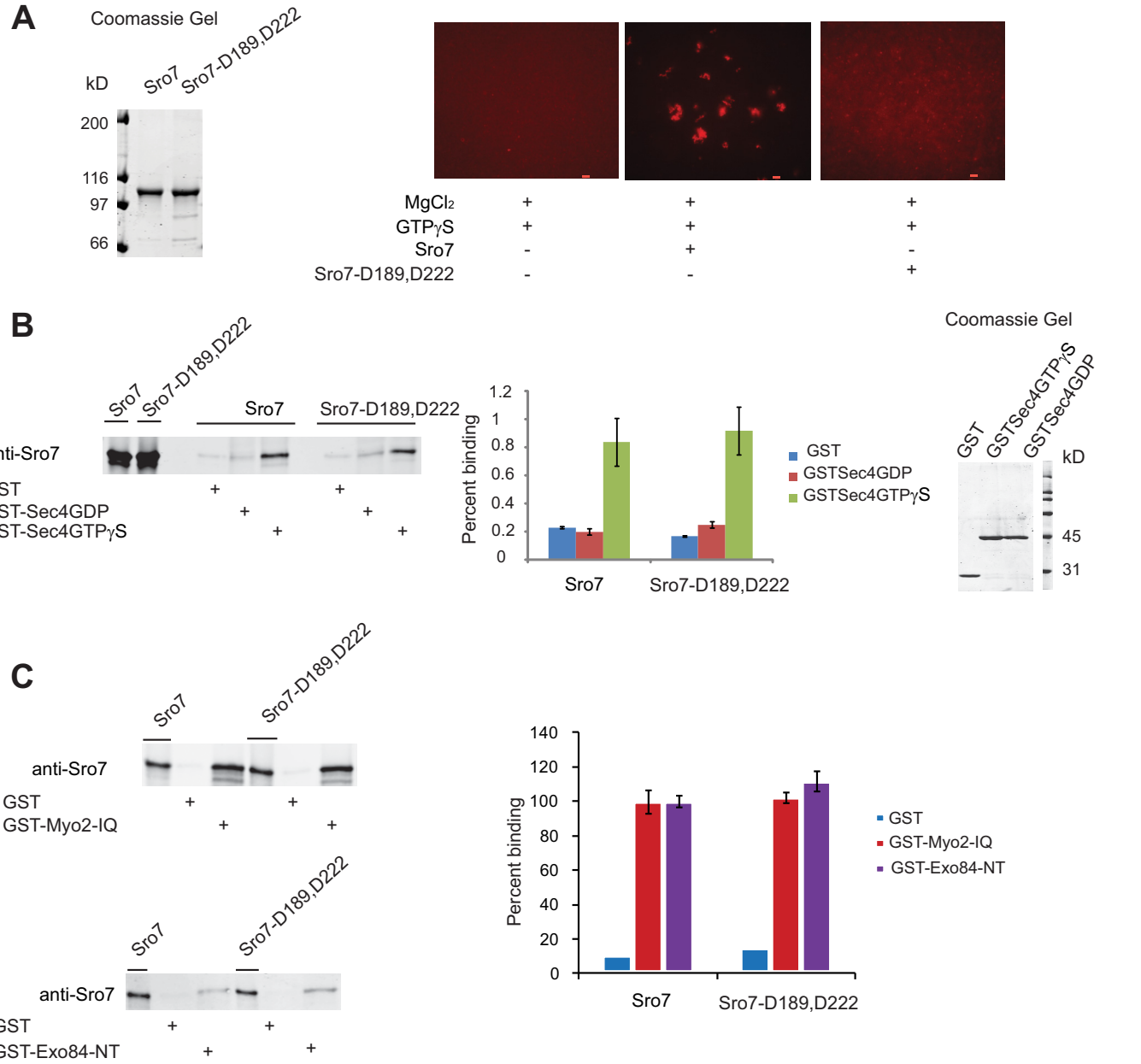

FIGURE 6. **Biochemical characterization of Sro7-D189,D222 shows that although the novel mutant cannot cluster vesicles in the *in vitro* clustering assay, it can still bind to Sec4-GTP, Myo2, and Exo84 in GST pulldown assays.** *A*, Sro7 and Sro7-D189,D222 were purified and analyzed at identical concentrations in the *in vitro* clustering assay. *Scale bar*, 2 μm. *B*, purified Sro7 and Sro7-D189,D222 also examined for binding to GST fusions of the Rab GTPase Sec4; *C*, IQ region of Myo2 (amino acids 782–990) and the N terminus of Exo84 (amino acids 3–400) by standard methods described previously. Percent binding in *C* was expressed using wild type Sro7 binding as 100%. All bindings represent the result of three independent experiments conducted with two different concentrations of GST fusion proteins on beads.

DISCUSSION

In this paper, we describe for the first time an *in vitro* system in which we recapitulate Rab-dependent post-Golgi vesicle/vesicle clustering induced by the yeast Lgl/tomosyn family member Sro7. We find that many of the features present in Sro7-mediated vesicle clustering *in vivo* and *in vitro* closely resemble vesicle tethering events that are thought to occur prior to fusion with the target membrane. The most important similarity is the requirement in both cases for GTP-bound Rab protein and a direct Rab effector in the formation of a close physical apposition of a vesicle with an opposing membrane. It has been previously suggested that this phenomenon might involve symmetric "pairing" of Rab-GTP molecules on both membranes, which may be stabilized by effector/Rab and effector/effector interactions (23). Certainly the dependence of the clustering assay and post-Golgi transport on Sec4-GTP and Sro7 supports this notion, although further biochemical dissection of this system will be required to distinguish the precise tethering mechanism involved.

Genetically and biochemically, Sro7 has features that suggest it likely functions parallel to the exocyst complex downstream of the Sec4 GTPase. Evidence for a parallel function to the exocyst complex includes direct GTP-dependent

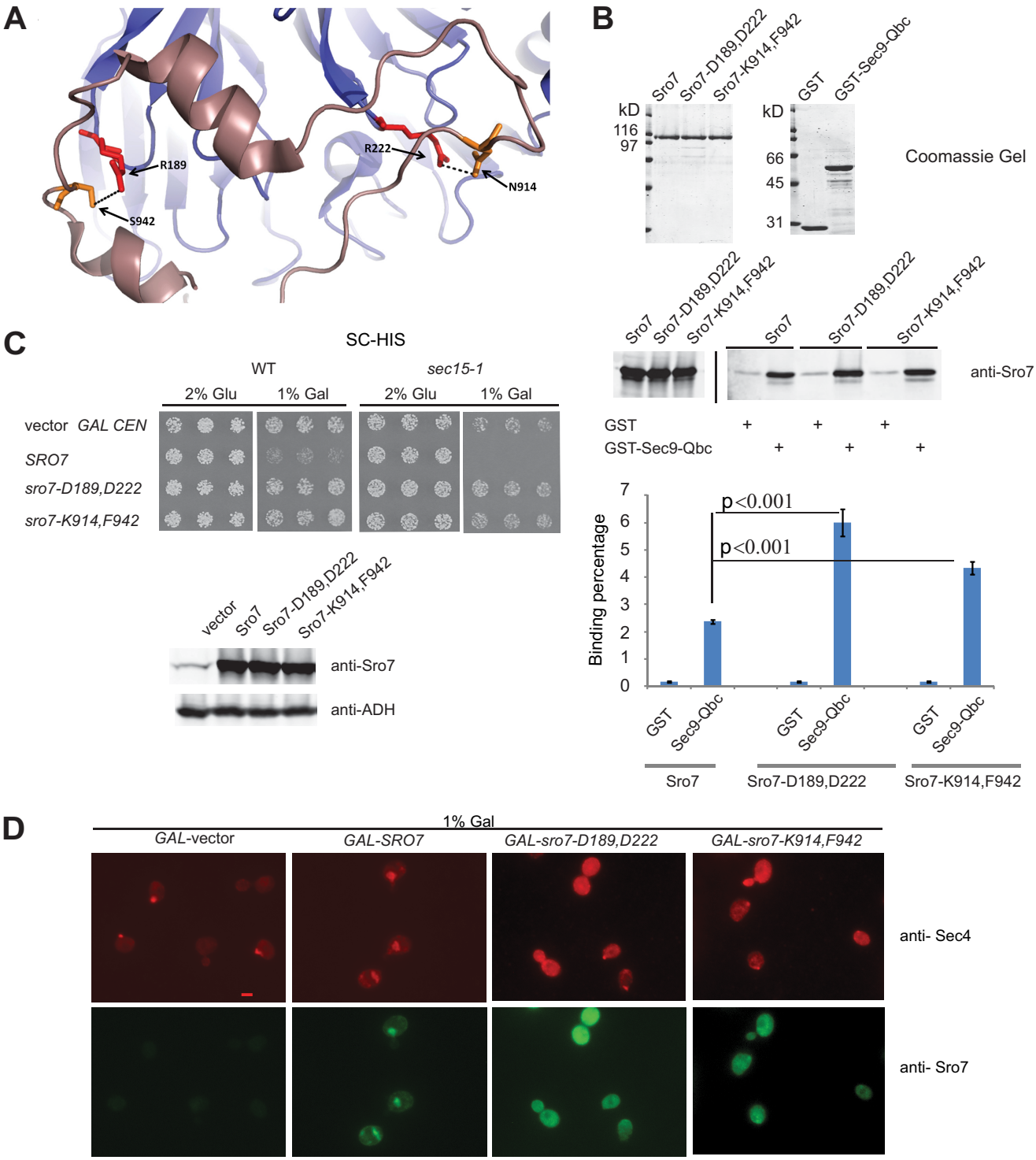

FIGURE 7. **Sro7-N914K,S942F behaves genetically and biochemically like sro7-R189D,R222D.** *A*, schematic structure of Sro7 illustrating hydrogen bonds between R189,R222 on the N-terminal propeller of Sro7 and N914,S942 on the C-terminal tail. *B*, wild type and mutant Sro7 proteins were purified and analyzed for binding to the Sec9-Qbc domain as described previously. Standard Student's *t* test showed a *p* value of <0.001. *C*, wild type and *sec15-1* mutant strains were transformed with plasmids (*CEN*) overexpressing *SRO7*, *sro7-D189,D222* and *sro7-K914,F942* from a *GAL* promoter. Three individual colonies were picked and transferred to selective media in the presence of glucose or galactose. Equal absorbance units of the strains induced in galactose were harvested, washed in Tris (10 mM) and azide (20 mM), and lysed by glass bead lysis before subjecting to Western blot analysis. *D*, wild type cells containing plasmids expressing Sro7, or mutant proteins from a *GAL*-inducible promoter (*CEN*), or vector only were grown in selective media and induced for 6 h in galactose before fixing and processing for immunofluorescence analysis using monoclonal Sec4 and polyclonal Sro7 antibodies. *Scale bar*, 2 μm.

binding to Sec4 (like the Sec15 component) and dosage suppression of a number of exocyst mutants, including bypass suppression of *exo70*Δ, *sec5*Δ, and *sec3*Δ (1, 2). However, because Sro7 also physically interacts with the Exo84 component of the exocyst complex, some aspects of its activity may be interdependent with the exocyst (3). In the assay described in this paper, it is clear that the tethering/clustering activity we observe for Sro7 is almost certainly independent

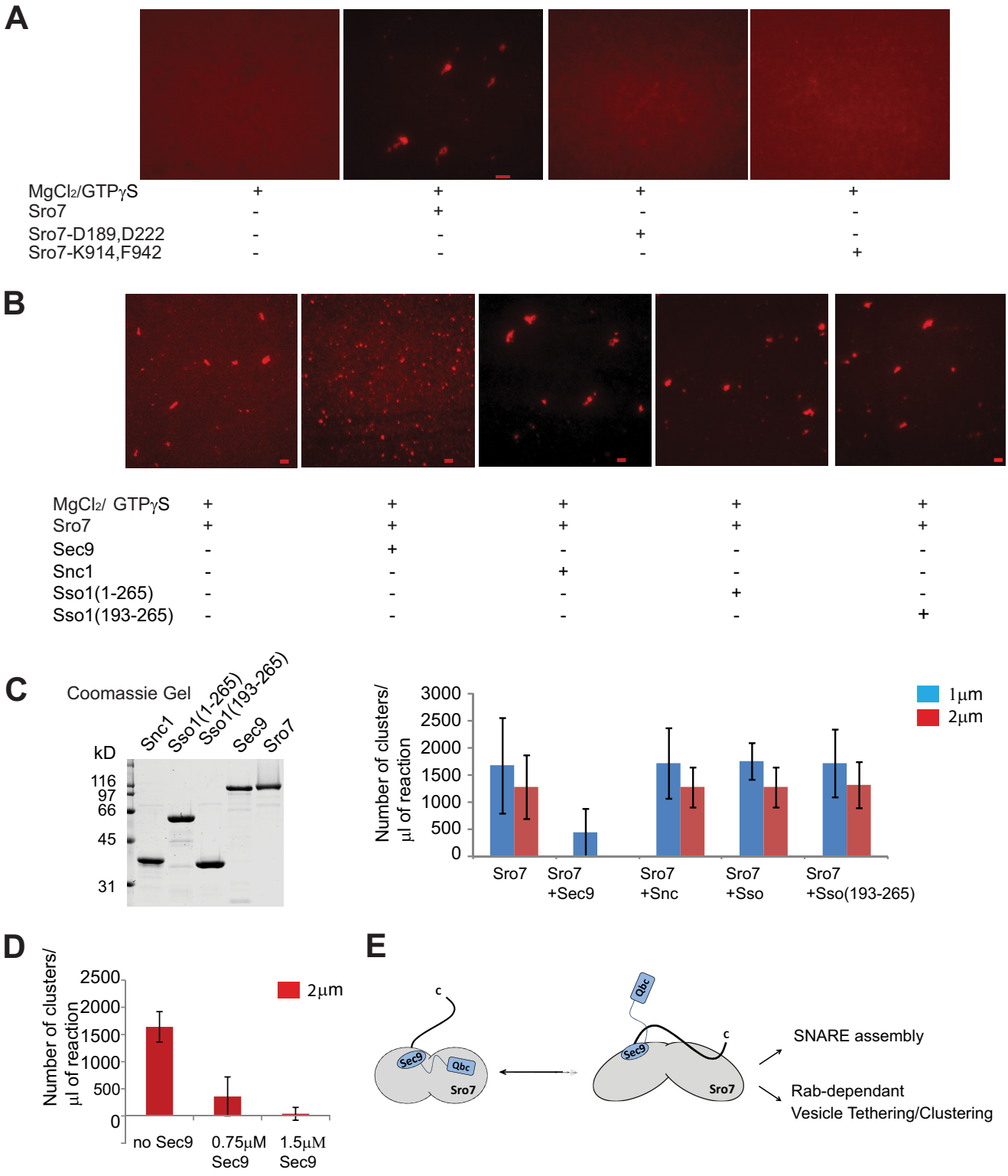

FIGURE 8. **Sro7 mutants that favor an open conformation inhibit Sro7-mediated vesicle clustering *in vitro*.** *A*, Sro7, Sro7-D189,D222 and Sro7-K914,F942 were purified and analyzed at identical concentrations in the *in vitro* clustering assay. *Scale bar*, 2 μm. *B*, *in vitro* clustering assay was performed with Sro7 (1.5 μM) or a mixture of Sro7 and Sec9 (1:1), Sro7 and GST-Snc (1:1), Sro7 and GST-Sso1 (1:1), or GST-Sso1 (amino acids 193–651) (1:1) previously incubated on ice for 60 min. The assay was analyzed and quantitated as described previously. Results of the quantitation and Coomassie stain of the proteins used is shown in *C*. *D*, inhibitory effect of Sec9 on Sro7 is dose-dependent. *E*, model showing how the closed conformation of Sro7 allows release of the Sec9-Qbc domain and Rab-dependent vesicle clustering to occur simultaneously.

of the exocyst, as this complex does not stably associate with vesicles and is absent from post-Golgi vesicles following the size-dependent purification method used in this work (24).

Previous structural analyses of the Rab effector Sro7 (5) strongly suggest that binding of the C-terminal autoinhibitory tail of Sro7 to the N-terminal propeller represents a molecular

switch in the function of this protein in vesicle transport. In this model, Sro7 would deliver the t-SNARE Sec9 to sites of fusion with the Sec9-Qbc domain bound to the N-terminal propeller and the autoinhibitory domain in the "open" conformation (see Fig. 8*E*). When the appropriate signal or trigger is present, the autoinhibitory domain would bind back to the N-terminal propeller, resulting in the release of the Sec9-Qbc domain. This would then allow the Sec9-Qbc domain to be available for assembly into active t-SNARE and trans-SNARE complexes required for vesicle fusion. Here, using two sets of point mutations shown to destabilize the autoinhibitory tail, we demonstrate that the conformational status of the tail plays a critical role in determining the activity of Sro7 in Sec4-dependent vesicle clustering. Although both regulation of the tail of Sro7 and the presence of Sec4-GTP are important for clustering *in vitro* and *in vivo*, Sec4 binding by itself does not appear to be the trigger for this conformational switch, because mutations that favor the open conformation show equivalent binding to Sec4-GTP.

Because Rab-dependent vesicle tethering to the appropriate membrane is thought to occur prior to the SNARE-mediated fusion, we expected that the open conformation of Sro7 would be most active in Rab-GTP-mediated vesicle clustering. The fact that we find exactly the opposite of this expectation, *i.e.* the open conformation is inactive, may be indicative of a quite different temporal relationship between Rab tethering and fusion. Instead of happening at quite discrete and sequential stages, these two events appear to be coincident in their regulation. This may help to ensure that neither Rab-mediated tethering nor SNARE-mediated fusion occur promiscuously with the wrong membrane by requiring an additional triggering interaction. We have previously described another "gating" interaction with the type V myosin Myo2, by which the interaction between Sro7 and Sec4 is regulated. Taken together, this suggests that Sro7 is well designed to orchestrate assembly and disassembly events on the surface of the post-Golgi vesicles that are critical for vesicle transport, tethering, and fusion. This may help to aid in increasing the overall spatial and temporal specificity of the transport events.

The development of the *in vitro* assay described here will be an important tool for further dissecting the mechanism by which Rab GTPases and their effectors function in transport. Further identification of protein/protein and protein/lipid interactions that are important for post-Golgi transport *in vivo* and vesicle clustering *in vitro* will allow specific models for the role of Sro7 in these processes to be tested.

Acknowledgments—We thank Dr. Leah Watson for critical reading of the manuscript; Dr. Vincent Starai for the pGDI-CDB plasmid; Dr. Jussi Jantti for the sso2-1 mutant strain; Dr. Jeff Gerst for the Snc1 GAL depletion strain; and Hal Mekeel and Dr. Joe Costello for invaluable assistance with electron microscopy.

REFERENCES

1. Lehman, K., Rossi G., Adamo J. E., and Brennwald, P. (1999) Yeast homologues of tomosyn and lethal giant larvae function in exocytosis and are associated with the plasma membrane SNARE, Sec9. *J. Cell Biol.* **146,** 125–140
2. Grosshans, B. L., Andreeva, A., Gangar, A., Niessen, S., Yates, J. R., 3rd, Brennwald, P., and Novick, P. (2006) The yeast lgl family member Sro7p is an effector of the secretory Rab GTPase Sec4p. *J. Cell Biol.* **172,** 55–66
3. Zhang, X., Wang, P., Gangar, A., Zhang, J., Brennwald, P., TerBush, D., and Guo, W. (2005) Lethal giant larvae proteins interact with the exocyst complex and are involved in polarized exocytosis. *J. Cell Biol.* **170,** 273–283
4. Rossi, G., and Brennwald, P. (2011) Yeast homologues of lethal giant larvae and type V myosin cooperate in the regulation of Rab-dependent vesicle clustering and polarized exocytosis. *Mol. Biol. Cell* **22,** 842–857
5. Hattendorf, D. A., Andreeva, A., Gangar, A., Brennwald, P. J., and Weis, W. I. (2007) Structure of the yeast polarity protein Sro7 reveals a SNARE regulatory mechanism. *Nature* **446,** 567–571
6. Salminen, A., and Novick P. J. (1989) The Sec15 protein responds to the function of the GTP binding protein, Sec4, to control vesicular traffic in yeast. *J. Cell Biol.* **109,** 1023–1036
7. Gangar, A., Rossi, G., Andreeva, A., Hales, R., and Brennwald, P. (2005) Structurally conserved interaction of Lgl family with SNAREs is critical to their cellular function. *Curr. Biol.* **15,** 1136–1142
8. Starai, V. J., Jun, Y., and Wickner, W. (2007) Excess vacuolar SNAREs drive lysis and Rab bypass fusion. *Proc. Natl. Acad. Sci. U.S.A.* **104,** 13551–13558
9. Brennwald, P., Kearns, B., Champion, K., Keränen, S., Bankaitis, V., and Novick, P. (1994) Sec9 is a SNAP-25-like component of a yeast SNARE complex that may be the effector of Sec4 function in exocytosis. *Cell* **79,** 245–258
10. Adamo, J. E., Rossi, G., and Brennwald, P. (1999) The Rho GTPase Rho3 has a direct role in exocytosis that is distinct from its role in actin polarity. *Mol. Biol. Cell* **10,** 4121–4133
11. Walch-Solimena, C., Collins, R. N., and Novick, P. J. (1997) Sec2p mediates nucleotide exchange on Sec4p and is involved in polarized delivery of post-Golgi vesicles. *J. Cell Biol.* **137,** 1495–1509
12. Novick, P., Field, C., and Schekman, R. (1980) Identification of 23 complementation groups required for post-translational events in the yeast secretory pathway. *Cell* **21,** 205–215
13. Walworth, N. C., and Novick, P. J. (1987) Purification and characterization of constitutive secretory vesicles from yeast. *J. Cell Biol.* **105,** 163–174
14. Goud, B., Salminen, A., Walworth, N. C., and Novick, P. J. (1988) A GTP-binding protein required for secretion rapidly associates with secretory vesicles and the plasma membrane in yeast. *Cell* **53,** 753–768
15. Protopopov, V., Govindan, B., Novick, P., and Gerst, J. E. (1993) Homologs of the synaptobrevin/VAMP family of synaptic vesicle proteins function on the late secretory pathway in *S. cerevisiae*. *Cell* **74,** 855–861
16. Jäntti, J., Aalto, M. K., Oyen, M., Sundqvist, L., Keränen, S., and Ronne, H. (2002) Characterization of temperature-sensitive mutations in the syntaxin 1 homologues Sso1p and Sso2p, and evidence of a distinct function for Sso1p in sporulation. *J. Cell Sci.* **115,** 409–420
17. Garrett, M. D., Zahner, J. E., Cheney, C. M., and Novick, P. J. (1994) GDI encodes a GDP dissociation inhibitor that plays an essential role in the yeast secretory pathway. *EMBO J.* **13,** 1718–1728
18. Ullrich, O., Stenmark, H., Alexandrov, K., Huber, L. A., Kaibuchi, K., Sasaki, T., Takai, Y., and Zerial, M. (1993) Rab GDP dissociation inhibitor as a general regulator for the membrane association of Rab proteins. *J. Biol. Chem.* **268,** 18143–18150
19. Forsmark, A., Rossi, G., Wadskog, I., Brennwald, P., Warringer J., and Adler, L. (2011) Quantitative proteomics of yeast post-Golgi vesicles reveals a discriminating role for Sro7p in protein secretion. *Traffic* **12,** 740–753
20. Mulholland, J., Wesp, A., Riezman, H., and Botstein, D. (1997) Yeast actin cytoskeleton mutants accumulate a new class of Golgi-derived secretary vesicle. *Mol. Biol. Cell* **8,** 1481–1499
21. Lipatova, Z., Tokarev, A. A., Jin, Y., Mulholland, J., Weisman, L. S., and Segev, N. (2008) Direct interaction between a myosin V motor and the Rab GTPases Ypt31/32 is required for polarized secretion. *Mol. Biol. Cell* **19,** 4177–4187
22. Novick, P., and Brennwald, P. (1993) Friends and family: the role of the Rab GTPases in vesicular traffic. *Cell* **75,** 597–601
23. Lo, S. Y., Brett, C. L., Plemel, R. L., Vignali, M., Fields, S., Gonen, T., and Merz, A. J. (2012) Intrinsic tethering activity of endosomal Rab proteins. *Nat. Struct. Mol. Biol.* **19,** 40–47
24. Bowser, R., and Novick, P. (1991) Sec15p, an essential component of the exocytic apparatus, is associated with the plasma membrane and with a soluble 19.5 S particle. *J. Cell Biol.* **112,** 1117–1131